Asian Journal of Physics
Vol. 33, Nos 3 & 4 (2024) 239-251
Available on: www.asianjournalofphysics.com

ap

On the optothermal properties of vanadium dioxide from the visible to the infrared

R Li Voti, M Bertolotti, G Leahu, E Petronijevic, G M Cesarini, M C Larciprete,
M Centini, A Belardini, F Bovino, and C Sibilia

Università di Roma La Sapienza-Dipartimento SBAI, Via Scarpa 16, 00161 Roma, Italy

Dedicated to Professor Anna Consortini for her significant contributions and pioneering works in the field of atmospheric turbulence and her continuous commitment to promote optics at global level

In this paper, we present an overview of results obtained during the last few years about optothermal properties of vanadium dioxide (VO_2) films, realized with different methods of deposition, and a variety of substrates. VO_2 is one of the most interesting materials exhibiting metal-insulator transitions, with a transition temperature of 340 K. We report the MIR and LWIR response of a number of VO_2 films, in particular we report the behavior of the thermal emissivity during the phase transition.

Doi: 10.54955/AJP.33.3-4.2024.239-251

Keywords: Infrared, Optothermal properties, Thermal emissivity, Vanadium dioxide.

1 Introduction

The thermochromic properties of vanadium dioxide (VO_2) have been deeply investigated since 1959, when Morin reported for the first time the evidence of the semiconductor-metallic phase transition (SMT) [1]. The attention given to the vanadium dioxide is due to its extraordinary feature of drastic changes of properties from the semiconductor state (rutile crystallographic structure) to the metallic state (monoclinic structure); electric properties such as electrical conductivity may change up to five orders of magnitude [2], and the optical properties widely vary during the SMT (first-order phase transition). This transition takes place at a critical temperature of $T_c \cong 68°C$, with a very narrow hysteresis if single crystal is analyzed. In synthesis, at high temperatures ($T > T_c$) vanadium dioxide exhibits metallic properties, showing a high electrical conductivity, and inhibiting the propagation of electromagnetic waves. On the contrary, at low temperatures ($T < T_c$), VO_2 behaves as a semiconductor, showing a relatively high transparency in the infrared spectral range [3].

Due to its phase transition as a function of the temperature, VO_2 has aroused a lot of interest for possible applications in infrared optical systems, smart windows, "smart" blackbody devices for spacecraft, light modulators just to mention a few of them. By doping VO_2 with other elements, for example tungsten, it is possible to change the phase transition temperature, bringing it to values close to room temperature (W-VO_2, with 1.9% of W, behaves like a semiconductor below $T_c = 302$ K (29°C), while for higher temperatures it is a conductor capable of providing a consistent reflectivity. The optical properties of VO_2 are dramatically changed during the phase change from semiconductor to metal. In particular, the scattering law of the complex index ($n+ik$) as a function of wavelength changes substantially, as can be seen in [4,5]. The behavior at high temperature becomes metallic with increase of the extinction coefficient. In thin films, an enlargement of the

Corresponding author
e mail: concita.sibilia@uniroma1.it (C Sibilia)

hysteresis loop is observed, which is due to the presence of a great number of nanocrystals with different sizes while the hysteresis loop of the polycrystal results from the sum of all the elementary hysteresis cycles in each nanocrystal [6]. It is possible to control the width of hysteresis loops, as well as speed of the SMT, that are both useful parameters for various applications. In the case of thin films for applications to optical devices operating in the infrared (IR) range, the IR properties of the substrate, where the VO_2 film is grown, are of first importance [7-9]. The possibility to manipulate the infrared signature in MIR range (3-5 μm), by using VO_2 based nanostructures, has been proposed for dual use purposes [10]. Structures more complex than thin films have also been considered. For example, in order to obtain a three-dimensional photonic band gap (PBG) with specific electrical and optical properties, refs. [11,12] reported the realization of synthetic opal-VO_2 composites made by self-assembled silica spheres where the pores among the spheres are partially filled with VO_2. Also, to realise a micro-optical shutter driven by an external voltage, W-doped VO_2 thin films have been used to decrease T_c [13].

The thermal hysteresis loop prevalent in phase transition processes has attracted increasing attention, and it was found to be affected by several factors such as the film deposition temperature [14], the wavelength range [15], the choice of suitable substrate [16,17], the use of metallic content [18] as well as the size of metallic phase domains [19]. Specifically, in [15], the hysteresis loop was investigated in both front and rear configurations, i.e. infrared radiation coming from the VO_2 layer and the substrate, respectively and was found to be considerably different in the two configurations. The thermal hysteresis was also investigated for thin films with different thicknesses showing a clear dependence of the transition temperature and the width of the hysteresis loop on the film thickness and on the size of the crystallites [14]. The hysteresis loop was also characterized across different wavelength ranges and it was shown that some wavelengths allow large transmittance variation in contrast to other wavelengths, where the tunability was extremely reduced [18]. Critical temperature range was also observed to depend on the operation wavelength, and it was attributed to the size of the metallic clusters created during phase transition [16]. In further investigations, doping is proven to affect and modify the hysteresis loop. For example, both the critical phase transition temperature and the hysteresis width were modified by doping VO_2 nanoparticles with Ti and W [17]. All of the investigated methods provide an array of parameters that allow the control of the phase transition characteristics such as smoothing temperature gradient, reducing hysteresis loop width, and varying the critical temperature. Thus, the obtained results on these lines of research are pivotal tools for designing, improving and customizing the performance of thermally tunable devices based on VO_2 thin films and nanostructures [14-25].

In this work, we review, both theoretically and experimentally, the tuning of infrared emission from VO_2 thin films in different configurations: on different substrates, in multilayers, and coupled with nanostructures. We focus on the 3.3-5.1 μm wavelength range. Within this wavelength range, we also provide experimental proof where we employ a highly emissive object placed below the sample to show different emission features arising at different heating/cooling rates. We evaluate and address the effects of the different contributions to the overall IR radiation and investigate the critical role of VO_2 as the active material for thermal emission tuning. We also comment on the dynamics of the VO_2 transition.

2 Experimental

In this work, we use a radiometric apparatus for VO_2 characterization. We discuss the measurements of IR transmittance and reflectance, integrated in the MIR region (2.5-5 μm), across the phase transition of two samples. Figure 1 shows the analyzed samples. Sample A is a VO_2 thin film (≈190 nm) deposited on a polished mirror-like silicon wafer; the wafer thickness and diameter are 480 μm and 100 mm, respectively. The VO_2 layer was deposited by means of reactive radio frequency sputtering with a substrate temperature of 500°C, and the layer thickness is determined by surface profilometry measurements. Sample B contains Cu layer, sandwiched between the two VO_2 layers (with the same substrate properties). Morphological aspects of samples are shown in Figs 2.

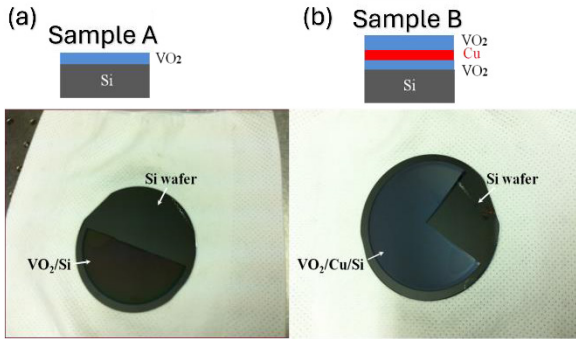

Fig 1. Schematics and photos of the two investigated samples. (a) Sample A contains a single layer of VO_2; (b) Sample B contains VO_2-Cu-VO_2 multilayer . The photos show that part of the substrate wafer has been left free of deposition so that it can be used as a reference for measurements [15].

In Fig 2, we show the characteristics of both the samples obtained by means of Scanning Electron Microscopy (SEM), and their roughness obtained by Atomic Force Microscopy (AFM).

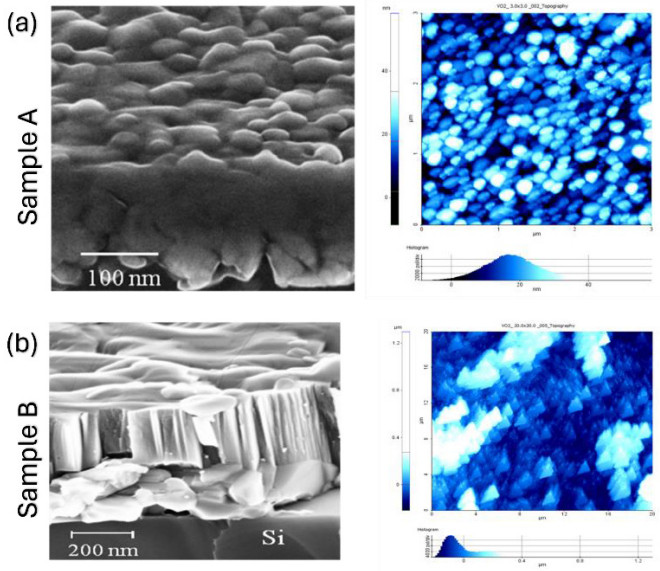

Fig 2. (a) Sample A: SEM image (left), and roughness obtained by AFM (right). (b) Sample B: SEM image (left), and roughness obtained by AFM (right).

The thermal hysteresis of the reflectance has been measured in the front configuration (R_f - reflectance from the VO_2 film side), and in the rear configuration (R_r -reflectance from the Si wafer side). Front emissivity (E_f) and rear emissivity (E_r) have been indirectly calculated on the basis of the experimental data of both reflectance (R_f, R_r) and transmittance T_r.

To measure transmittance and reflectance, a Globar lamp IR source was kept at a temperature of about 500°C and was modulated by a mechanical chopper before reaching the sample under test. For the reflectance measurement, the IR radiation reflected by the sample was first detected by a (HgCdZn)Te photovoltaic IR detector (Vigo System model PVI-5, quadrant cells 2×2 mm^2) with a high and rather flat sensitivity in the MIR range (2.5-5.0 μm), and detected signal was then measured with a lock-in amplifier. In order to perform the MIR transmittance measurements as a function of sample temperature, a central hole of 10 mm in diameter was realized in the copper body of the electrical heater used for the sample temperature scan. The

current temperature of the sample was measured by a copper-constantan thermocouple, and, in view of the low sample heat capacity, thin electrical wires of 0.05 mm in diameter (type TG-40-T, NYThermoelectric Co. Inc) were used to minimize the heat losses from the contact points of the thermocouple. The temperature scan of the sample was performed in a quasi stationary regime, realized by changing linearly the sample temperature slowly with time, with a low speed of about1°C/min. A germanium lens is placed at the distance 2F (F=50 mm is the focal length) from both the sample surface and the detector so that the image of the investigated zone of the sample was projected to the active zone of the detector with a magnification 1:1.

In temperature-dependent emission measurements, the Globar source was not used for phase transition characterization. In this configuration, as shown in Fig 3, the mechanical chopper is placed between sensor and sample and near the latter, in such a way as to modulate (36 Hz) the emittance coming from the structure under examination, and a diaphragm is placed following the chopper to let pass only the radiation coming from the sample area whose image is in correspondence with the active zone of the detector. While the temperature scan was performed in the usual range 30 – 100 °C, we performed the detection in SWIR, LWIR and MIR bands. This type of measurement is more affected by error due to environmental noise that can be modulated by the chopper and therefore be synchronous with the input frequency of the lock-in.

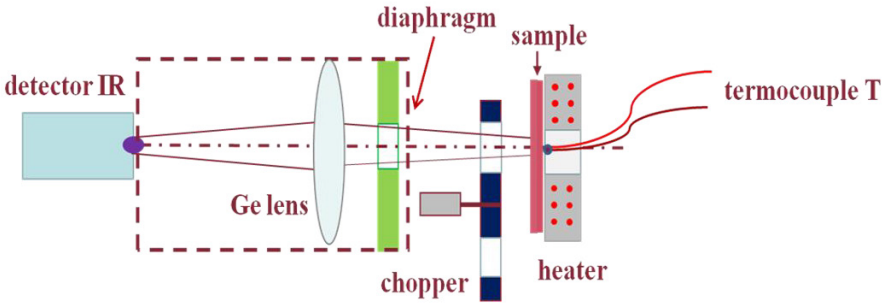

Fig 3. Schematization of the experimental setup for emission measurements as a function of temperature.

3 Results and Discussion

The optical properties of VO_2 are sharply changed during the phase semiconductor-to-metal transition; thus, the dispersion law of the complex refractive index $n + ik$ is strongly modified [26]. In general, the performance of either optical and thermal switches can be quantified and estimated through the so-called dynamic range, which is the difference between the largest and smallest possible values of the MIR data as a function of the temperature. Within the present work, we define this figure of merit as the difference between the emissivity values, averaged in the IR range 3-5 μm and calculated for two different regimes, i.e. below and above T_c . Given this assumption, the sign of the dynamic range completely changes the filter behavior and thus determines the type of application. A thermochromic filter displaying positive dynamic range, i.e. an IR emissivity decreasing with increasing temperature, is suitable for IR signature reduction as well as for smart windows for thermal control [7]. On the other hand, a negative dynamic range is required for space applications and emissivity control of spacecraft [27]. As explained above, many experimental and theoretical works have shown that the thermal emissivity variation with temperature of VO_2 thin films is strongly influenced by the substrate used for the deposition. In what follows, apart from the measurements, we consider simulations of the optical response of VO_2 thin films first deposited on different substrates, and then in multilayer structures, below and above the T_c. We discuss the effect of different substrates as well as VO_2 layer thicknesses on the sign of the dynamic range. Finally, we introduce metallo-dielectric multilayer structures, composed of alternating copper or silver and VO_2 layers, where the layer thickness is systematically varied in order to further increase and optimize the dynamic range.

Material properties of VO_2

In 1959, the scholar F J Morin announced the discovery of a semiconductor-metal transition in vanadium dioxide [1]. The first theoretical description of the transition dynamics of VO_2 was given by Goodenough [3], who explained that the electrical properties of the material were closely related to the transition and changed precisely as a function of it. When VO_2 is heated beyond its phase transition temperature (T_c), its structure changes from monoclinic to tetragonal in a very short time (of the order of hundreds of femtoseconds); the schematic of this process is shown in Fig 4. This brings the vanadium atoms closer together: the bond that is created between the two metal atoms increases in intensity as the overlap of the wave functions of the bond orbitals increases. As a result of this change in the binding orbitals, energy levels change.

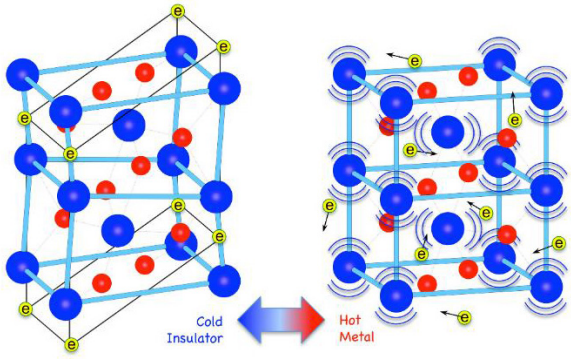

Fig 4. Structure of vanadium dioxide in the two phases monoclinic – insulating (left) and tetragonal–conductive (right). Vanadium atoms are indicated in blue and oxygen atoms in red. In the high temperature phase, the vibration of vanadium atoms allows electrons to delocalize and vanadium atoms to settle symmetrically.

When VO_2 is in the semiconducting monoclinic phase, the approach of vanadium atoms and the overlap of their orbitals cause the 3d orbitals to split into two energy levels, one full and one empty (in accordance with the electronic structure of vanadium: [Ar]3d). This induces a further spacing of energy levels, which leads to the opening of a band-gap of about 0.7 eV. As already mentioned, the phase transition is also accompanied by large changes in the electrical, thermal and optical properties of the material. The magnitude of the variation depends strictly on the characteristics of the sample (bulk, thin film, powder) and how it is prepared. This variation is identified as a first-order phase transition. This means that the electrochemical potential, the derivative before the Gibbs potential, is a function of temperature that has a discontinuity in T_c. We can then describe the function of the Gibbs potential with μ_1 before the discontinuity and μ_2 after. The characteristic equation for a first-order phase transition is therefore:

$$\left(\frac{\partial \mu_1}{\partial T}\right)_P\Big|_{T_c} \neq \left(\frac{\partial \mu_2}{\partial T}\right)_P\Big|_{T_c} \tag{1}$$

The variation of the electrochemical potential involves a discontinuous change of several physical properties, including conductivity and reflectivity, in the surroundings of the critical temperature, and thus explains the discontinuous effects found.

We next present some of the most relevant results obtained by means of radiometric apparatus in the spectral range of IR. Although the IR spectrum extends from red light to microwave radiation, i.e. 0.77 to 1000 μm, there are only two wavelength ranges showing high IR transmittance in the atmosphere, i.e. 3-5 and 8-12 μm, known as the mid (MWIR) and long (LWIR) IR windows, respectively. In that spectral range, we present the work done on VO_2 thin films. Samples have been realized by using different substrates and in

different configurations showing as radiometric apparatus allow to obtain information about the emissivity parameter. Emissivity is a fundamental parameter able to qualify the properties of VO_2 as material to be utilized in applications where tunability of the optical properties are required.

3.2 Thermal emissivity and tunable VO_2 thin film

A study for the design and optimization of the VO_2 films may start from the calculation of the emissivity of VO_2thin films on several different substrates with varying film thickness. As well-known from Kirchhoff's law, the directional spectral emittance is equal to the directional spectral absorptance so that $\varepsilon = 1 - R - T$, where R and T, respectively are the reflectance and transmittance of the structure.

To compare the different structures one fundamental quality factor to be introduced is the tunability of emissivity defined as the difference of the emissivity of the cold film minus the emissivity of the hot film. This quantity is usually averaged over the narrow window of the particular infrared camera [λ_{min} to λ_{max}] (in our example the MWIR window 3-5 μm) as follows [28]:

$$\Delta\varepsilon_{av} = \frac{\int_{\lambda_{min}}^{\lambda_{max}} \Delta\varepsilon\, d\lambda}{\lambda_{max} - \lambda_{min}} = \frac{\int_{\lambda_{min}}^{\lambda_{max}} (\varepsilon_c - \varepsilon_h)\, d\lambda}{\lambda_{max} - \lambda_{min}} \tag{2}$$

where ε_c, ε_h correspond respectively to the emissivity of the filter when cold or hot with respect to the transition temperature. Figure 5 shows the average tunability of the emissivity ε_{av} as a function of the VO_2 thickness. The curves refer to different substrates with optical properties taken from the literature: infrared transparent substrates (CaF_2: blue curve [29]. Si: pink curve [30]), infrared opaque or metallic substrate (copper: black curve [31]), and as a reference, a hypothetical free standing VO_2 film in air (red curve). The emissivity is here calculated as $\varepsilon = 1 - R - T$ for normal incidence by using transfer matrix method. In the figure the inset shows the behaviour at small VO_2 thickness (micron).

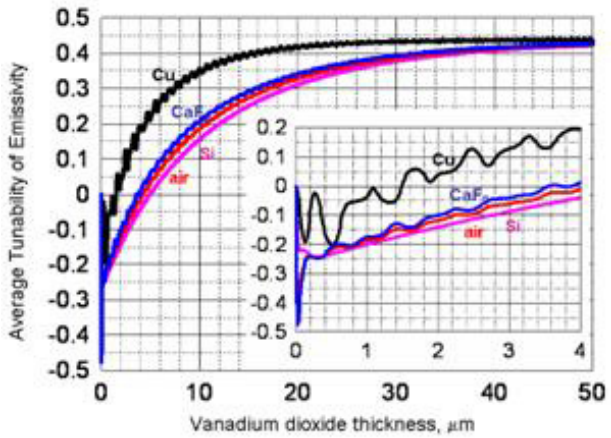

Fig 5. Average tunability of emissivity vs the vanadium dioxide thickness for different substrates: copper (black line), silicon (pink line), calcium fluoride (blue line), none (red line). Inset: magnification of the small vanadium dioxide thickness range.

The average tunability of emissivity might change sign on varying the vanadium dioxide thickness d_{VO_2}. For example, in the case of the VO_2/CaF_2 system (blue dotted line in Fig 6), the average tunability reaches a minimum value of about $\varepsilon_{av} = -0.4$ for $d_{VO_2} = 20$ nm (thin layer), while for thick layers it changes sign giving $\varepsilon_{av} > +0.3$ for $d_{VO_2} = 20$ μm.

The emissivity of the sample with the thin VO_2 layer (20 nm) increases with temperature (see dotted lines: blue for ε_c, red for ε_h), while the reverse happens for the sample with the thick VO_2 layer (20 μm) (see

solid lines: blue for ε_c, red for ε_h). In this last case interference fringes also appear in both MWIR and LWIR (blue solid line). The periodicity of the oscillation is of the order of the wavelength, and the vanadium dioxide is in the semiconductor state.

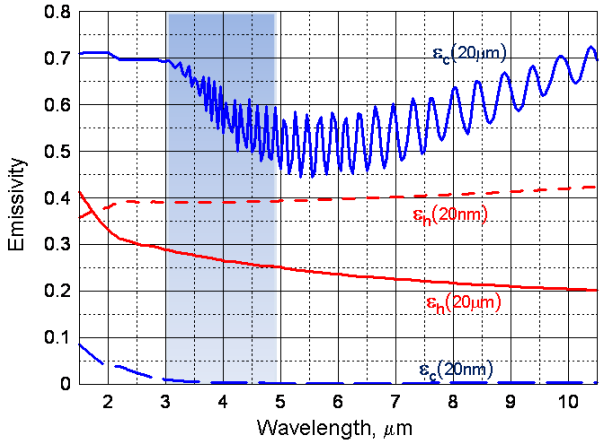

Fig 6. Cold and hot emissivity spectra of VO_2/CaF_2 for both thin and thick vanadium dioxide thicknesses. Cold 20μm layer (blue solid line); hot 20 μm layer (red solid line); cold 20 nm layer (blue dotted line); cold 20nm layer (red dotted line).

In order to design an IR tunable filter the requirement is to work with a structure with a large and positive tunability, $\varepsilon_{av} > 0$. This is achieved by increasing the film thickness (see Fig 5), and also by using metallic absorbing substrates able to enhance the whole cold emissivity ε_c when VO_2 is in the semiconducting state. The black curve in Fig 5, corresponding to a copper substrate, shows an enhancement of the tunability up to the limiting value of $\varepsilon_{av} = +0.45$. Similar behaviour is seen when using other metallic substrates.

We may now ask if it is possible to achieve a further enhancement of the tunability by using a more complex structure which uses vanadium dioxide and metal layers. Therefore, we study how to enhance the tunability of a single VO_2 film by designing an optimized VO_2/Metal multilayer structure acting as a tunable transparent metal. Transparent metals basically are 1D photonic band gap (PBG) multilayers which exhibit passband properties in the optical range. This unusual and rare property of transparency for metals is achieved by growing an adequate sequence of metal thin layers (≈10 nm) and transparent dielectric thick layers. Thanks to the tunnelling phenomena in the metal layers and the interference effects in the dielectric layers, these structures are able to enhance the transmittance at some wavelengths.

After some preliminary tests, we have chosen to optimise a structure shown in Fig 7, which satisfies the following requirements:

(a) It is made up of an odd number N of layers. A number of (N+1)/2 VO_2 layers are alternated with a number of (N–1)/2 metallic layers.
(b) The two outer vanadium dioxide layers have the same thickness $d_{ext}VO_2$.
(c) The inner vanadium dioxide layers have the same thickness $d_{int}VO_2$.
(d) Each metal layer (Cu or Ag) is 10 nm thick so as to guarantee optical tunnelling.

Although this structure does not maximize the number of degrees of freedom (i.e. thicknesses of the different layers), it is sufficiently flexible. An example of an optimization is reported below for a VO_2/Cu structure made of N = 9 layers. The 4 layers of Cu are 10 nm thick. Simulations were made by changing the VO_2 thicknesses of both the inner layers of thickness d_{intVO_2} and outer layers of thickness d_{extVO_2} in the range 0-500 nm. The tunability of the emissivity for each layer pair $[d_{intVO_2}, d_{extVO_2}]$ has been estimated. The maximum of $\varepsilon_{av} = +0.53$ is reached when $d_{intVO_2} = 370$ nm and $d_{extVO_2} = 230$ nm. The second example in Fig 7

(right) shows the optimization for the same VO_2/Cu structure but with a very large number of layers (N = 21) in order to check if any asymptotic limit for the obtainable value of ε_{av} exists. The maximum of the average emissivity is now $\varepsilon_{av} = +0.67$ for $d_{intVO_2} = 420$ nm and $d_{extVO_2} = 230$nm. As N increases there is an increase of ε_{av} and an adjustment of d_{intVO_2} which finally stabilizes to 420 nm.

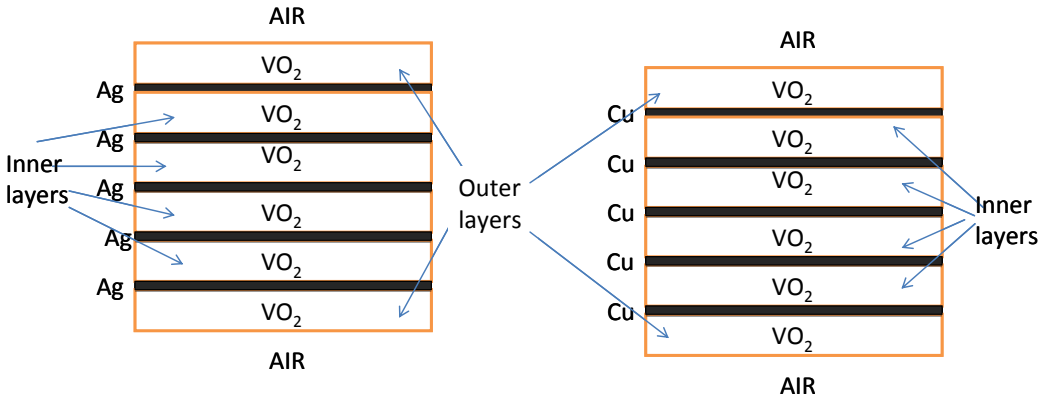

Fig 7. Sketch of the VO_2/Ag and VO_2/Cu multilayers structures. The number of layers is here for example N = 7.

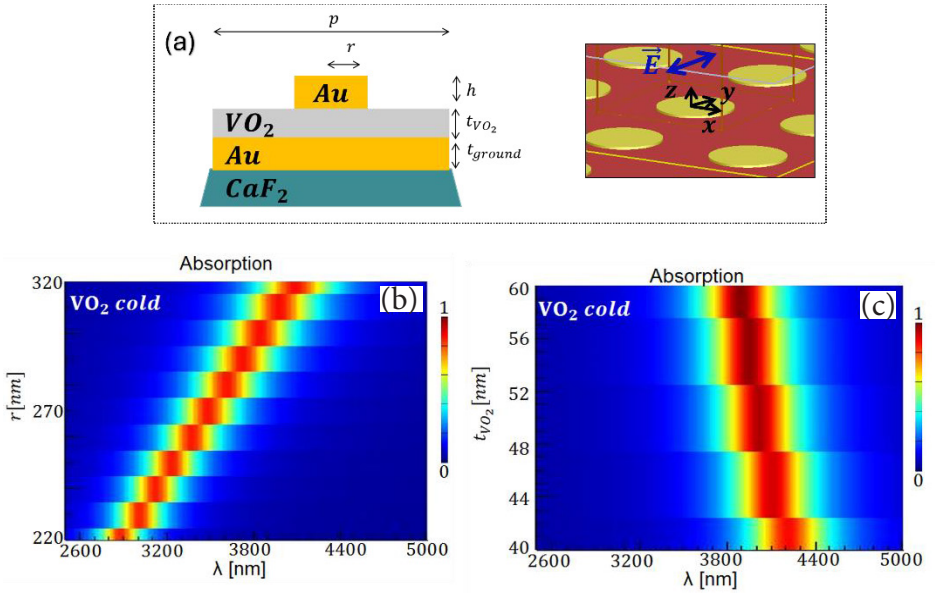

Fig 8. (a) Sketch of the Au/VO_2/Au/CaF_2 metamaterial which strongly absorbs below the transition temperature. (b) The spectral position of the absorption peak is prevalently defined by the nanodisc radius. (c) The absorption peak also depends on the thickness of VO_2, thus requesting for special care during the fabrication.

VO_2 can be used in combination with metamaterial geometries, to provide designs for active tuning of the optical properties in the desired wavelength range [10,32,33]. Below, we show that a simple, plasmonic gap geometry can be combined with a thin layer of VO_2, in order to obtain resonant behaviour in 3-5 μm range. The schematic in Fig 8(a) shows a thin layer of VO_2 sandwiched between a golden nanoresonator and golden substrate layer; the whole metamaterial lies on a CaF_2 substrate, and, when VO_2 is metallic, it strongly reflects the light. Therefore, in the "hot" state, the absorption (and the emissivity) is expected to be negligible. When the VO_2 is below the phase transition, its semiconductor nature allows for a gap-plasmon resonance,

the peak of which can be tuned by changing the geometry. In Fig 8(b), we see that the Au nanodisc radius strongly defines the position of the absorption peak; other parameters are p = 1000 nm, h = 30 nm, t_{VO_2} = 40 nm, t_{ground} = 80 nm, n_{VO_2} = 2.3, n_{CaF_2} =1.4. However, if we fix the radius (e.g. to r =330 nm) and change the VO_2 thickness, this can also influence the spectral position of the resonance, as it can be appreciated from Fig 8(c). Therefore, special care should be taken during the VO_2 deposition of the exact thickness.

Finally, taking into account all previous theoretical and numerical considerations, we experimentally investigate the samples shown in Fig 2. These samples were realized by sputtering VO_2 onto the substrates. Figure 9 reports the emissivity for Sample, in various spectral ranges, along with the table with the calculated difference in the emissivity. In Fig 10, same is shown for Sample B. It is evident that this sample provides great contrast in the SWIR range. Another remarkable detail is that our measurements indicate a variability of the radiative emission as a function of temperature as the spectral band of detection varies, and this demonstrates how the measurements made through a very slow temperature scan allow to extrapolate relevant details.

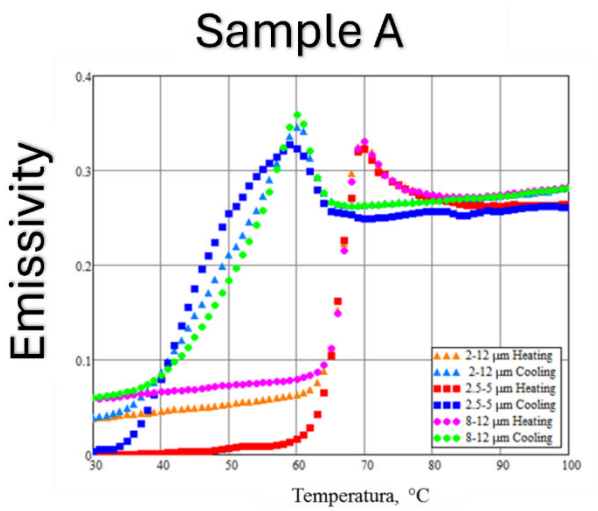

Spectral range [µm]	Tc (°C)		ΔTc (°C)	$\Delta\varepsilon_{HL}$
	Heating	Cooling		
SWIR (2.5 - 5)	66	43,5	22,5	0,26
MIR (3 - 12)	67	55,5	11,5	0,24
LWIR (8 - 12)	67	56,5	10,5	0,22

Fig 9. Emissivity hysteresis of Sample A in different IR spectral ranges.

3.3 Dymanics of the transition

Regarding the dynamics of the transition from semiconductor to metal, several papers report a very fast dynamics. One of early studies by Cavalleri [34] in 2001 reports the reflectivity of a 200-nm film of VO_2 laid on glass investigated as a function of irradiation by an 800 nm wavelength laser with pulses of 50 fs. The system adopted is a pump-probe type, and the changes in VO_2 properties are obtained for the first time in a photoinduced manner and not in a thermal one.

Measurements were made as a function of laser fluence (the energy of the single pulse of light sent on the sample per unit area). At the fluence of 63mJ/cm^2, irreversible damage of VO_2 by ablation is observed. From the dynamic measurements we get that with the fluence of 7mJ/cm^2 the transition time is around 46ps, with the fluence of 15mJ/cm^2 the time is shorter, 420 fs, while with the fluence of 25mJ/cm^2 there is the time of 100 fs, which is at the limit of instrumental resolution.

In the previous studies, it was seen that the temperature transition exhibits a hysteresis loop. This hysteresis has been interpreted as an effect of the dispersion of the size of the transiting domains due to the granularity of the crystallization. This effect has been verified very precisely [35] for 108-nm films of VO_2 on rutile (TiO_2).

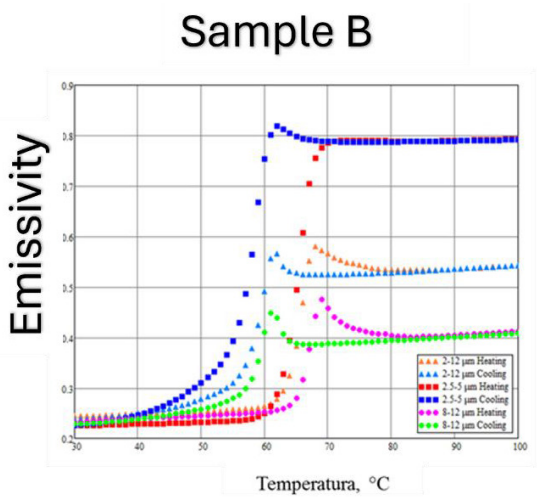

Spectral range [μm]	Tc (°C)		ΔTc (°C)	$\Delta\varepsilon_{HL}$
	Heating	Cooling		
SWIR (2.5 - 5)	65	0,50	7	0,57
MIR (3 - 12)	65,5	0,50	6	0,30
LWIR (8 - 12)	67	0,49	8	0,18

Fig 10. Emissivity hysteresis of Sample B in different IR spectral ranges.

To study the phase transition of VO_2, nonlinear optical properties, such as third harmonic generation, were also investigated. The transition is studied by measuring the change in third harmonic intensity as a function of both temperature and pump laser intensity.

The sample under measurement is a single crystal of VO_2 and the laser used pulses 50fs (at 10nJ per pulse) at a wavelength of 1250 nm. The fluence that allows a photoinduced transition a of about 10mJ/cm^2, while the damage threshold is about 60mJ/cm^2.

From the measurements, it was observed that the intensity of the third harmonic increases by a factor of 30 in the transition between the insulating state of VO_2 and the conductive state. This fact makes it clear that the increase in the third harmonic signal cannot be explained in terms of the change in the linear optical properties of the crystal, but precisely by a change in the crystal structure reflected in a change in the third-order nonlinear tensor $\chi^{(3)}$. In addition, one can see how much more sensitivity there is in investigating the transition by nonlinear measurements than by linear ones. The dependence of the third harmonic with the cube of the pump intensity was observed, which ensures that we are observing a $\chi^{(3)}$ process and not multi-photon luminescences, also we can see how the effect of the transition in VO_2 can be obtained in a photoinduced manner at the fluence threshold of 10mJ/cm^2. In the same paper, it was verified that the photoinduced transition is not due to temperature accumulation over time, but to the energy delivered within the single pulse of light, thus ensuring that the dynamics of the transition occurs in times less than 50fs. In the same work, an attempt was also made to measure the second harmonic, but the results were not reported. This is due to the fact that both crystallographic states of the two VO_2 phases are centrosymmetric and therefore do not exhibit a $\chi^{(2)}$ of 'bulk' [36].

Interestingly, in [37], photoinduced transition measurements, with lasers of 100fs at 790 nm, on films (50 nm and 200 nm) of VO_2 deposited on Si (111) are obtained for a threshold of 40mJ/cm^2 and damage at 80mJ/cm^2 instead of the lower values obtained on sapphire substrates. This is due to the effect of the higher thermal conductivity of silicon compared to sapphire, which dissipates some of the laser energy. However, the transition speeds are in line with the timelines obtained in the previous examples. In particular, the measurements of the reflectivity change at 790nm performed on a 50nm film present an estimated transition time of 90fs, while the thicker sample has and estimated the first time constant of 100fs.

The same sample of VO_2 (50 nm) on Si was subjected to photoinduced transition measurements (with fluence of 50mJ/cm^2) with femtosecond pulses of different durations from 1500 fs to 15f s with central

wavelength of 650 nm .The measurements show a structural limit to the response rate of about 75 fs for this sample type.

Nonlinear measurements in [38] also included the nonlinear absorption coefficient of a crystalline film of VO_2 (210 nm) on silicon oxide, using the transmission Z-scan technique (open aperture Z-scan) for measurements made at a temperature of 22°C. The fluence used (pump laser at 800 nm, 120 fs, 1kHz) is about 2mJ/cm^2, so well below the transition threshold. We see a decrease in transmission as intensity increases corresponding to a nonlinear absorption coefficient b = 270 cm/GW. Due to the high reflectivity at high temperatures (100 °C), the absorption in the conductive phase is negligible, and the measurement of the nonlinear coefficient in the conductive phase is estimated to be lower in modulus at 1cm/GW.

In the same paper, through the closed aperture Z-scan, the nonlinear coefficient of refraction g = –7.1cm^2/W at 22°C and g = +7.5 cm^2/W at 100 °C was also measured, where the change of sign between insulating and conductive phase is noted. Measurements were also repeated on a sample of VO_2 nanocrystals (nanorods) on silicon oxide. In that sample, it was interesting to observe the extreme width of the hysteresis curve, due to the polycrystalline nature of the nanorods, compared to the crystalline film. The coefficients g and b are related, respectively, to the real and imaginary part of the third-order nonlinear term $\chi^{(3)}$.

The transition speed also depends on the substrate-induced crystalline orientation effect, as shown in [39]. In this article, time-dependent phase transition was measured for VO_2 films (30 nm) deposited on different substrates: amorphous quartz (SiO_2), R-oriented sapphire (Al_2O_3) (012), C-oriented sapphire (Al_2O_3) (001). The phase transition is investigated in a photoinduced manner, with a pump-probe technique where the pump (400 nm laser, 130 fs) is divided into two equal beams (total fluence 30mJ/cm^2) and made to interfere on the sample. This forms a diffraction grating formed by alternating conductive and insulating strips.

It was seen that the response times of VO_2 vary from 450 fs on amorphous substrates (the VO_2 film results with a poor crystallographic orientation), up to 140fs for R-oriented sapphire, where the crystallographic orientation of VO_2 film was improved.

4 Conclusions

In this paper, we report experimental and numerical results on the opto-thermal properties of VO_2 under different configurations; moreover, we also comment on dynamic response of the transition as reported in the literature. Opto-thermal properties of VO_2 and its combination in various geometries is still an active field of research, with prospective applications. Moreover, new results by improved methods of deposition and on different substrates will surely open new perspectives in VO_2-based micro- and nano-technology.

References

1. Morin F J, Oxides which show a metal-to-insulator transition at the Neel temperature, *Phys Rev Lett*, 3(1959)34.
2. Kucharczyk D, Niklewski T, Accurate X-ray determination of the lattice parameters and the thermal expansion coefficients of VO_2 near the transition temperature, *J Appl Cristallogr*, 12(1979)370; doi.org/10.1107/S0021889879012711.
3. Goodenough J B, The two components of the crystallographic transition in VO_2, *J Solid Chem*, 3(1971)490–500.
4. Guinneton F, Sauques L, Valmalette J C, Cros F, Gavarri J R, Optimized infrared switching properties in thermochromic vanadium dioxide thin films: role of deposition process and microstructure, *Thin Solid Films*, 446(2004)287–295.
5. Leahu G, Li Voti R, Sibilia C, Bertolotti M, Anomalous optical switching and thermal hysteresis during semiconductor-metal phase transition of VO_2 films on Si substrate, *Appl Phys Lett*, 103(2013)231114; doi.org/10.1063/1.4838395.
6. Shadrin E B, Il'inskii A V, Sidorov A I, Khanin S D, Size effects upon phase transitions in vanadium oxide nanocomposites, *Phys Solid State*, 52(2010)2426–2433.

7. Brassard D, Fourmaux S, Jean-Jacques M, Kieffer J C, Khakani M A, Grain size effect on the semiconductor-metal phase transition characteristics of magnetron-sputtered VO_2 thin films, *Appl Phys Lett*, 87(2005)051910; doi.org/10.1063/1.2001139.
8. Narayan J, Bhosle V M, Phase transition and critical issues in structure-property correlations of vanadium oxide, *J Appl Phys*, 100(2006)103524; doi.org/10.1063/1.2384798.
9. Benkahoul M, Chaker M, Margot L, Haddad É, Kruzelecky R, Wong B, Jamroz W, Poinas P, Thermochromic VO2 film deposited on Al with tunable thermal emissivity for space applications, *Sol Energy Mater Sol Cells*, 93(2011) 3504–3508.
10. Petronijevic E, Sibilia C, Thin films of phase change materials for light control of metamaterials in the optical and infrared spectral domain, *Opt Quantum Electron*, 52(2020)110; doi.org/10.1007/s11082-020-2237-6.
11. Kurdyukov D A, Grudinkin S A, Nashchekin A V, Smirnov A N, Trofimova E Y, Yagovkina M A, Pevtsov A B, Golubev V G, Melt synthesis and structural properties of opal-V_2O_5 and opal-VO_2 nanocomposites, *Phys Solid State*, 53(2011)428–434.
12. Hendaoui A, Émond N, Chaker M, Haddad É, Highly tunable-emittance radiator based on semiconductor-metal transition of VO_2 thin films, *Appl Phys Lett*, 102(2013)061107; doi.org/10.1063/1.4792277.
13. Soltania M, Chaker M, Haddad E, Kruzelecky R, Margot J, Laou P, Paradis S, Fabrication of stationary micro-optical shutter based on semiconductor-to-metallic phase transition of W-doped VO_2 active layer driven by an external voltage, *J Vac Sci Technol*, A26(2008)763–767.
14. Ramirez-Rincon J A, Gomez-Heredia C L, Corvisier A, Ordonez-Miranda J, Girardeau T, Paumier F, Champeaux C, Dumas-Bouchiat F, Ezzahri Y, Joulain K, Ares O, Alvarado-Gil J J, Thermal hysteresis measurement of the VO_2 dielectric function for its metal-insulator transition by visible-IR ellipsometry, *J Appl Phys*, 124(2018)195102; doi.org/10.1063/1.5049747.
15. Cesarini G, Leahu G, Belardini A, Centini M, Li Voti R, Sibilia C, Quantitative evaluation of emission properties and thermal hysteresis in the mid-infrared for a single thin film of vanadium dioxide on a silicon substrate, *Int J Therm Sci*, 146(2019)106061; doi.org/10.1016/j.ijthermalsci.2019.106061.
16. Cesca T, Scian C, Petronijevic E, Leahu G, Li Voti R, Cesarini G, Macaluso R, Mosca M, Sibilia C, Mattei G, Correlation between in situ structural and optical characterization of the semiconductor-to-metal phase transition of VO_2 thin films on sapphire, *Nanoscale*, 12(2020)851–863.
17. Li Voti R, Leahu G, Larciprete M C, Sibilia C, Bertolotti M, Photothermal characterization of thermochromic materials for tunable thermal devices, *Int J Thermophys*, 36(2015)1004–1015.
18. Okada M, Takeyama A, Yamada Y, Thermal hysteresis control of VO_2 (M) nanoparticles by Ti-F codoping, *Nano-Struct. Nano-Objects*, 20(2019)100395; doi.org/10.1016/j.nanoso.2019.10039.
19. Liang J, Hu M, Kan Q, Liang X, Wang X, Li G, Chen H, Infrared transition properties of vanadium dioxide thin films across semiconductor-metal transition, *Rare Metals*, 30(2011)247–251.
20. Mercuri F, Orazi N, Paoloni S, Cicero C, Zammit U, Pulsed thermography applied to the study of cultural heritage, *Appl Sci*, 7(2017)1010; doi.org/10.3390/app7101010.
21. Orazi N, Mercuri F, Zammit U, Paoloni S, Marinelli M, Giuffredi A, Salerno C S, Thermographic analysis of bronze sculptures, *Stud Conserv*, 61(2016)236–244.
22. Larciprete M C, Centini M, Paoloni S, Fratoddi I, Dereshgi S A, Tang K, Wu J, Aydin K, Adaptive tuning of infrared emission using VO_2 thin films, *Sci Rep*, 10(2020)11544, doi.org/10.1038/s41598-020-68334-2.
23. Larciprete M C, Centini M, Paoloni S, Dereshgi S. A, Tang K, Wu J, Aydin K, Effect of heating/cooling dynamics in the hysteresis loop and tunable IR emissivity of VO_2 thin films, *Opt Express*, 28(2020)39203–39215.
24. Li Voti R, Larciprete M C, Leahu G, Sibilia C, Bertolotti M, Optical response of multilayer thermochromic VO_2-based structures, *J Nanophotonics*, 6(2012)061601; doi.org/10.1117/1.JNP.6.061601
25. Kocer H, Butun S, Banar B, Wang K, Tongay S, Wu J, Aydin K, *Sci Rep*, 5(2015)13384; doi.org/10.1038/srep13384.
26. Kats M A, Blanchard R, Zhang S, Genevet P, Ko C, Ramanathan S, Capasso F, Vanadium dioxide as a natural disordered metamaterial: perfect thermal emission and large broadband negative differential thermal emittance, *Phys Rev X*, 3(2013)041004; doi.10.1103/PhysRevX.3.041004.

27. Leahu G, Li Voti R, Larciprete M C, Belardini A, Mura F, Fratoddi I, Sibilia C, Bertolotti M, AIP Conf Proc 1603 (2014)62–70.
28. Li Voti R, Larciprete M C, Leahu G, Sibilia C, Bertolotti M, Optimization of thermochromic VO_2 based structures with tunable thermal emissivity, *J Appl Phys*, 112(2012)034305; doi.org/10.1063/1.4739489.
29. Malitson I H, A redetermination of some optical properties of calcium fluoride, *Appl Opt*, 2(1963)1103–1107.
30. Palik E D (ed), Handbook of optical constants of solids, (Academic Press, Inc. New York), 1985.
31. Foiles C L, Landolt and Bornstein, Group III: Condensed Matter, Vol.15b: Electronic Properties- Metals: Electronic Transport Phenomena-Electrical Resistivity, Thermoelectrical Power and Optical Properties, V. 43A11 (2012); doi. 10.1007/978-3-642-22847-6.
32. Seo M, Kyoung J, Park H, Koo S, Kim H S, Bernien H, Kim B J, Ho Choe J, Ahn Y H, Kim H.-T, Park N, Park Q-H, Ahn K, Kim D-S, Active Terahertz Nanoantennas Based on VO_2 Phase Transition, *Nano Lett*, 10(2010)2064–2068.
33. Petronijevic E, Centini M, Cesca T, Mattei G, Bovino F, Sibilia C, Control of Au nanoantenna emission enhancement of magnetic dipolar emitters by means of VO_2 phase change layers, *Opt Express*, 27(2019)24260–24273.
34. Cavalleri A, Tóth C, Siders C W, Squier J A, Ráksi F, Forget P, Kieffer J C, Femtosecond Structural Dynamics in VO_2 during an Ultrafast Solid-Solid Phase Transition, *Phys Rev Lett*, 87(2001)237401; doi.org/10.1103/ PhysRevLett.87.237401.
35. Petrov G I, Yakovlev V V, Squier J A, Nonlinear optical microscopy analysis of ultrafast phase transformation in vanadium dioxide, *Opt Lett*, 27(2002)655–657.
36. Leroux C, Nihoul G, Tendeloo G, From $VO_2(V)$ to $VO_2(R)$: Theoretical structures of polymorphs and *in situ* electron microscopy, *Phys Rev B*, 57(1998)5111; doi.org/10.1103/PhysRevB.57.5111.
37. Cavalleri A, Dekorsy Th, Chong H H W, Kieffer J C, Schoenlein R W, Evidence for a structurally-driven insulator-to-metal transition in : A view from the ultrafast timescale, *Phys Rev B*, 70(2004)161102; doi.org/10.1103/ PhysRevB.70.161102.
38. Lopez R, Haglund R F(Jr), Feldman L C, Optical nonlinearities in VO_2 nanoparticles and thin films, *Appl Phys Lett*, 85(2004)5191–5193.
39. Lysenko S, Vikhnin V, Fernandez F, Rua A, Liu H, Photoinduced insulator-to-metal phase transition in crystalline films and model of dielectric susceptibility, *Phys Rev B*, 75(2007)075109; doi.org/10.1103/PhysRevB.75.075109.

[*Received*: 29.02.2024; *accepted*: 30.03.2024]

Prof Roberto Li Voti is the Head of the Photothermal and Photoacoustic Laboratory at the Sapienza University of Rome, Italy. He is expert in photothermal deflection techniques, photothermal and photoacoustic spectroscopy, photothermal radiometry and infrared thermography for the nondestructive and quality testing of materials. He also has expertise in thermal diffusivity, optical and thermal depth profiling, detection of buried layers, and in the nondestructive testing of photovoltaic, nanophotonic, nanophononic and nanoplasmonic materials, in trace gas analysis, and in bioactive molecule detection.
e mail:roberto.livoti@uniroma1.it

Emilija graduated from the University of Belgrade (Serbia), in Physical Electronics, in 2014, as a valedictorian. She then did a Ph D at La Sapienza University of Rome under the supervision of Prof Sibilia. During her Ph D, she studied the interaction of light with plasmonic, dielectric and hybrid nanostructures, focusing on the numerical calculations of extrinsic chiro-optical response and on phase-change materials. During her Postdoctoral period, Emilija focused on the experimental work in the same fields. Emilija's current interest lies in chiral properties at the nanoscale, directed towards novel chiro-optical functionalities and the improved sensitivity of chiral sensing. She is a visiting researcher at the University of Bath, under the supervision of Prof Valev. e mail: emilija.petronijevic@uniroma1.it

Maria Cristina Larciprete is associate professor at Engineering Faculty of Sapienza University of Rome (Italy), where she is PI of the Materials and Metamaterials Infrared Laboratory (META-IR). She graduated in materials engineering at Sapienza University of Rome after experimental research activity using photothermal radiometry at the Institut für Optik und Quantenelektronik of Friedrich Schiller Universität Jena (De). She obtained a Ph D in materials engineering in 2003 with an experimental thesis on nonlinear optical materials for optical limiting applications. After post-doctoral activity in nonlinear optics and second order nonlinear optical materials, she moved towards the study of IR radiation manipulation, including the control of IR radiation polarization and/or temporal and spatial coherence. More recently her research is aimed at investigation of polar metamaterials and metasurfaces with tailored spectral response to set the basis for the realization of tunable and dynamically controllable systems as building blocks for the development of platforms for MIR functionalities including IR sensors and sources.
She is incharge of teaching activity for the following classes: General Physics, Physics I (Mechanics and Thermodynamics), Physics II (Electromagnetism), Physics Laboratory, for Engineering Faculty of Sapienza University of Rome since 2005 to date.
e mail: mariacristina.larciprete@uniroma1.it

Dr Alessandro Belardini is an Associate Professor in Experimental Physics at the Department of Basic and Applied Sciences for Engineering at Sapienza University of Rome. He received the Ph D degree in Physics at the University of Roma Tre in 2005. His actual research activities rely on the characterization of the chiral properties of self-assembled plasmonic metasurfaces. In particular, by using the second harmonic generation and photoacoustic signals. He is co-author of over 100 technical and scientific papers published in physics oriented International Journals. During his research activity, he developed a long-lasting experience in the experimental characterization of linear and nonlinear optical properties of different materials in cw and femtosecond regime. The investigations rely mainly on second harmonic generation in nanoplasmonic materials, metallo-dielectric nanostructures, hybrid organic metallo-dielectric nanostructures, optical delay line and nonlinear interaction in femtosecond regime, characterization of the electro-optic properties of organic molecules, photorefractive solitons. He participated as Speaker to many international conferences, more than ten of them as Invited. He is Member of the Board of the Directors of the European Optical Society (EOS), he is a Presidential Council Representative in SIOF, the Italian branch of EOS. He organised international conferences and schools in Plasmonics and Nanooptics.
e mail: alessandro.belardini@uniroma1.it

Concita Sibilia received her doctoral degree with honors in Physics from the University of Roma “La Sapienza”. She is currently at the Dipartimento di Scienze di Base e Applicate per l’Ingegneria (SBAI) of the University of Roma. She is full professor in Physics since 2000. She has been Director of the II level Master in “Optics and Quantum Information” at La Sapienza. The main research interests are in the field of optics, nonlinear optics at the nanoscale. She is responsible of many national and international projects. She is author of more than 650 papers, with more than 100 invited presentations at International Conferences. She is fellow of the American Optical Society and member of the European Physical Society.
concita.sibilia@uniroma1.it